THE ARCHIVE OF MECHANICAL ENGINEERING

VOL. LVII 2010 Number 2

10.2478/v10180-010-0006-y

**Key words:** motion control, multibody dynamics, flexible body, genetic algorithm, tether, Absolute Nodal Coordinate Formulation

*MOHD A. ABDULLAH* [*] *YOHEI MICHITSUJI* [**] *SHOICHIRO TAKEHARA* [***]
*MASAO NAGAI* [*], *NAOKI MIYAJIMA* [*]

# SWING-UP CONTROL OF MASS BODY INTERLINKED FLEXIBLE TETHER

One of the applications of tether system is in the field of satellite technology, where the mother ship and satellite equipment are connected with a cable. In order to grasp the motion of this kind of tether system in detail, the tether can be effectively modeled as flexible body and dealt by multibody dynamic analysis. In the analysis and modeling of flexible body of tether, large deformation and large displacement must be considered. Multibody dynamic analysis such as Absolute Nodal Coordinate Formulation with an introduction of the effect of damping force formulation can be used to describe the motion behavior of a flexible body. In this study, a parameter identification technique via an experimental approach is proposed in order to verify the modeling method. An example of swing-up control using the genetic algorithm control approach is performed through simulation and experiment. The validity of the model and availability of motion control based on multibody dynamics analysis are shown by comparison between numerical simulation and experiment.

## 1. Introduction

One of the applications of tether system is in the field of satellite technology, where the mother ship and satellite equipment are connected with a cable [1]. Information and data from the equipment to mother ship and vice versa are transmitted through the cable. The same cable is also used for support while keeping the equipment in free motion. In such a situation,

[*] *Department of Mechanical Systems Engineering Tokyo University of Agriculture and Technology, 2-24-16 Naka-cho, Koganei-shi, Tokyo 184-8588 Japan; E-mails: 50008833209@st.tuat.ac.jp, nagai@cc.tuat.ac.jp, 50006643120@st.tuat.ac.jp, web page: http://www.tuat.ac.jp/~mech/english/index.html*

[**] *Department of Mechanical Engineering Ibaraki University, 4-12-1 Nakanarusawa-cho, Hitachi-shi, Ibaraki 316-8511 Japan; E-mail: mitituji@mx.ibaraki.ac.jp*

[***] *Institute of Industrial Science (IIS) The University of Tokyo, 4-6-1 Komaba, Meguro-ku, Tokyo 153-8505 Japan; E-mail: stakeha@iis.u-tokyo.ac.jp*

it is essential to consider the motion control of the tether system. In order to grasp the motion of this kind of tether system in detail, the tether can be effectively modeled as a flexible body and dealt with multibody dynamic analysis [2, 3]. In addition, the kinematics control may be applied to the precise model of the tether for advanced machine application.

In the analysis and modeling of flexible body of tether, large deformation and large displacement must be considered. Multibody dynamic analysis such as Absolute Nodal Coordinate (ANC) Formulation can be used to describe the motion behavior of flexible body [4, 5]. It represents the coordinate of joint elements and the gradients using absolute coordinate system. The improvement of ANC is performed by introducing the effect of damping force and the effect of external drag force [6].

In the previous research, the modeling of flexible body of tether system verified the propriety of the ANC method concerning large deformation with consideration of Rayleigh damping force and elastic force [6, 7]. Furthermore, the tether system is a combination of rigid and flexible bodies as validated by numerical and experimental results [8].

Currently, there is no research on the identification technique for the damping parameter and drag coefficient. The damping parameter and drag coefficient produce significant effect on the behavior of tether. In this study, a parameter identification technique through an experimental approach is proposed. The damping parameter, which depends on the tether material and the drag coefficient are introduced in the analysis model of the tether. The damping parameter and drag coefficient, is produced from comparison of experimental and numerical results. The number of the element of the tether is decided for precise modeling and to shorten the simulation time.

The swing-up control of the mass object utilized the genetic algorithm (GA) approach. The fundamental of kinematics control for advanced machine [9] is considered on the tether tension application. The swing-up control experiment is performed based on control rule and practicality of the analytic model. The effectiveness of kinematics control of multibody dynamics using genetic algorithm is shown in comparison between numerical and experimental results.

## 2. Procedure of construction of analytical model and swing-up control rule formation

Fig. (1) shows the flow chart of multibody dynamic analysis and motion control of the tether system for numerical model and actual system. The first part is the construction of the parameter identification procedure and the second part is the motion control approach. After the analysis, a model is

constructed, and kinematics control is formed. These procedures are verified through an identification experiment and swing-up experiment, respectively. In this research, the tether model takes into consideration the damping force in the beginning of model formulation. The characteristic of the damping force depends on the unknown parameters. These unknown parameters and the number of element partitions are identified by comparison of experimental and numerical analysis results through evaluation function. The precise model is constructed by formulation from identification technique. The model utilizes the swing-up control rule with mass object connected to the tether end point. The genetic algorithm is used to track the movement pattern of the mass. The control rule formed in the simulation is transferred to the apparatus. The practicality of tether model is reflected by the apparatus where it captures the swing up of the mass object. The effectiveness of kinematics control of multibody dynamics is examined.

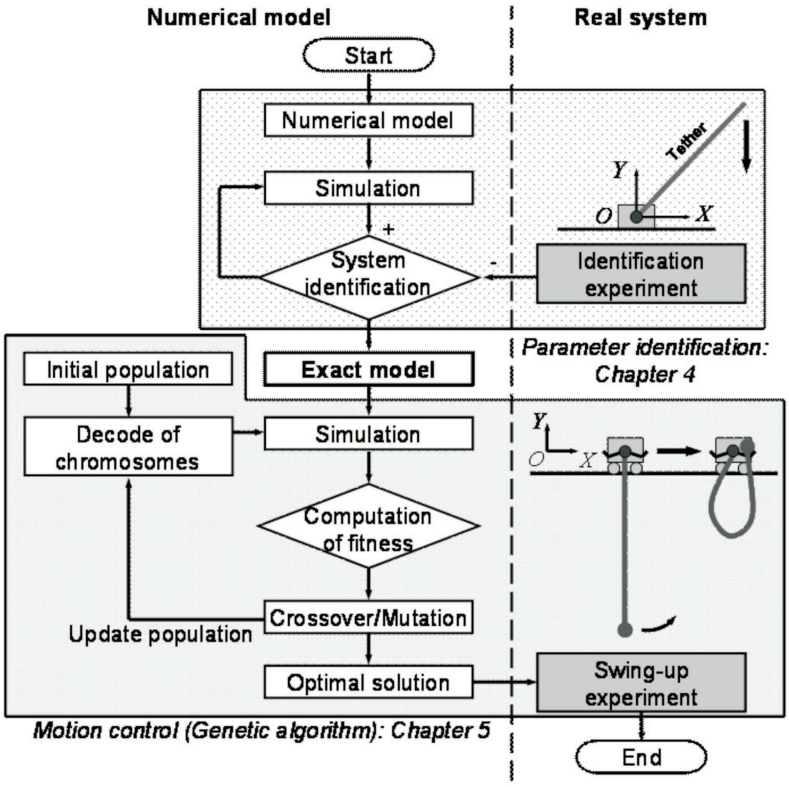


Fig. 1. Flow chart of motion control based on multibody dynamics model

## 3. Tether model with damping force consideration

In the modeling of the tether, the ANC formulation is utilized, the damping force is considered as an internal effect and drag force of air during tether movement is considered as external effect.

### 3.1. Formulation of tether

The experiment is designed so that one end of the tether is moved freely and the other is fixed. The motion of the tether is assumed to be in one surface $XY$ plane. In the previous research, the formulation of tether model using ANC method considered the elastic mass matrix and tether height, for shorter operation time [7]. Fig. (2) illustrates one element of the tether in absolute coordinate system. $OA$ and $O'A'$ are the tether conditions before and after deformation respectively. The position vector $\mathbf{r_a}$ is a function of shape function $\mathbf{S_a}$ and element vector $\mathbf{e}$ as shown in the following equation,

$$\mathbf{r_a} = \begin{bmatrix} r_x & r_y \end{bmatrix}^T = \mathbf{S_a} \cdot \mathbf{e} \tag{1}$$

Here, element vector e is the absolute coordinate of the entire nodal system,

$$\mathbf{e} = [\ e_1 \quad e_2 \quad e_3 \quad e_4 \quad e_5 \quad e_6 \quad e_7 \quad e_8\ ]^T \tag{2}$$

Where, $e_1, e_2$ is the $XY$ coordinate and $e_3, e_4$ is the slope of the beam at point $O'$. Similarly, $e_5, e_6$, and $e_7, e_8$ are the $XY$ coordinate and slope at point $A'$. The shape function $\mathbf{S_a}$ is defined as,

$$\mathbf{S_a} = \begin{bmatrix} \mathbf{S_1} \\ \mathbf{S_2} \end{bmatrix} = \begin{bmatrix} 1-3\xi^2+2\xi^3 & y\left(-6\xi+6\xi^2\right)/l_e \\ -y\left(-6\xi+6\xi^2\right)/l_e & 1-3\xi^2+2\xi^3 \\ l_e\left(\xi-2\xi^2+\xi^3\right) & y\left(1-4\xi+3\xi^2\right) \\ -y\left(1-4\xi+3\xi^2\right) & l_e\left(\xi-2\xi^2+\xi^3\right) \\ 3\xi^2-2\xi^3 & y\left(6\xi-6\xi^2\right)/l_e \\ -y\left(6\xi-6\xi^2\right)/l_e & 3\xi^2-2\xi^3 \\ l_e\left(\xi^3-\xi^2\right) & y\left(3\xi^2-2\xi\right) \\ -y\left(3\xi^2-2\xi\right) & l_e\left(\xi^3-\xi^2\right) \end{bmatrix}^T \tag{3}$$

Here, $\xi = x/l_e$ and $l_e$ is the length of one element. The kinetic energy of the element is,

$$T = \int_0^{l_e} \int_{-\frac{h}{2}}^{\frac{h}{2}} \frac{1}{2} \rho_t \dot{\mathbf{r}}_\mathbf{a}^T \dot{\mathbf{r}}_\mathbf{a} dy dx = \frac{1}{2} \dot{\mathbf{e}}^T \mathbf{M} \dot{\mathbf{e}} \tag{4}$$

**M** is the mass matrix of the element,

$$\mathbf{M} = \int_0^{l_e} \int_{-\frac{h}{2}}^{\frac{h}{2}} \rho_t \mathbf{S}_\mathbf{a}^T \mathbf{S}_\mathbf{a} dy dx \tag{5}$$

For the elastic force of the tether, the axial strain energy is denoted by the following equation,

$$U_l = \frac{1}{2} \int_0^{l_e} Ea\varepsilon^2 dx \tag{6}$$

Here, $\varepsilon$ is the axial strain of $O'A'$ and the elastic force is the partial differential of axial strain energy to element nodal coordinate vector **e**,

$$\mathbf{F_l} = \left( \frac{\partial U_l}{\partial \mathbf{e}} \right)^T \tag{7}$$

The bending energy $U_t$ due to bending deformation is described as,

$$U_t = \frac{1}{2} \int_0^{l_e} EI\kappa^2 dx \tag{8}$$

Here, $\kappa$ is the curvature of the point $P$. The partial differential of Eq. (8) gives elastic force due to bending energy,

$$\mathbf{F_t} = \left( \frac{\partial U_t}{\partial \mathbf{e}} \right)^T \tag{9}$$

The total elastic force of the tether is,

$$\mathbf{F_a} = \mathbf{F_l} + \mathbf{F_t} \tag{10}$$

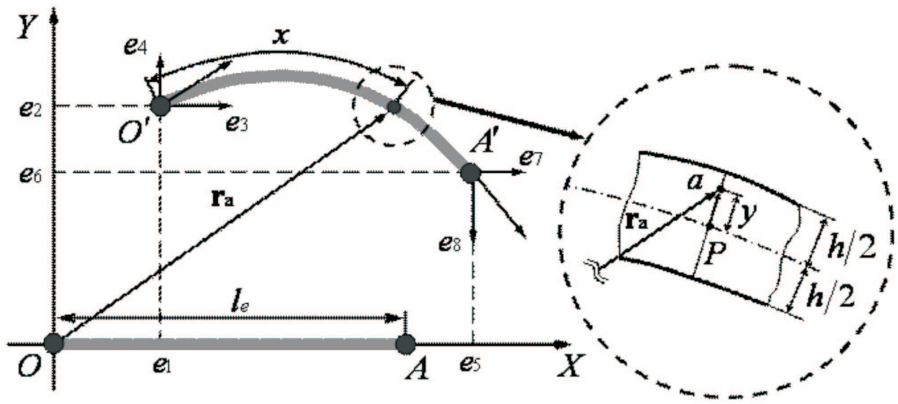


Fig. 2. Element of tether

In addition, the gravity acting on the tether can be written as,

$$\mathbf{Q} = \rho_t \cdot a \cdot l_e \cdot g \left[ \begin{array}{cccccccc} 0 & -\frac{1}{2} & 0 & -\frac{l_e}{12} & 0 & -\frac{1}{2} & 0 & \frac{l_e}{12} \end{array} \right]^T \tag{11}$$

### 3.2. Formulation of damping force

Since the tether is a flexible body, certain changes in damping will affect its behavior. However, ordinary ANC method does not consider the effect of damping. The damping force of the tether is derived from axial strain energy and bending deformation energy. The axial strain energy $U_{lD}$ is shown as,

$$U_{lD} = \frac{1}{2} \int_0^{l_e} D \cdot a \cdot \dot{\varepsilon}^2 dx \tag{12}$$

Here, $D$ is the newly introduced damping parameter. The damping force $\mathbf{F_{lD}}$ is defined as,

$$\mathbf{F_{lD}} = \left( \frac{\partial U_{lD}}{\partial \dot{\mathbf{e}}} \right)^T \tag{13}$$

The bending deformation energy $U_{tD}$, due to bending deformation, is denoted by,

$$U_{tD} = \frac{1}{2} \int_0^{l_e} D \cdot I \cdot \dot{\kappa} dx \tag{14}$$

And the damping force $\mathbf{F_{tD}}$, due to bending deformation, is computed by,

$$\mathbf{F_{tD}} = \left( \frac{\partial U_{tD}}{\partial \dot{\mathbf{e}}} \right)^T \tag{15}$$

The total damping force of the tether is,

$$\mathbf{F_D} = \mathbf{F_{lD}} + \mathbf{F_{tD}} \tag{16}$$

### 3.3. Formulation of damping force

In actual tether system, a significant resistance of movement exists in terms of drag force in the atmosphere. The drag force acting on each element of tether is represented in the drag force equation. Fig. (3) displays the

schematic diagram of the drag force acting on the tether. The drag force formula $Q_D$ with relative to velocity $v$, is defined in the following equation,

$$Q_D = C_D \cdot a \frac{\rho \cdot v^2}{2} \tag{17}$$

Where, $C_D$ is the drag coefficient, $a$ is the cross section area and $\rho$ is the density of air.

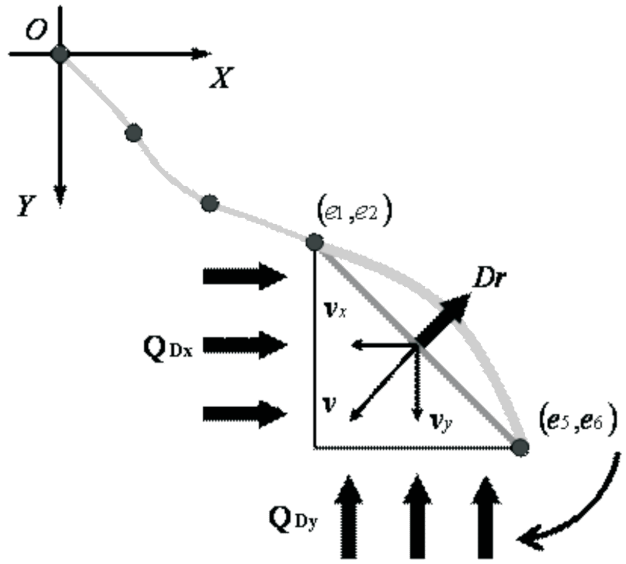


Fig. 3. Effect of drag

The deformation of the tether element is small and the component velocities $v_x$ and $v_y$ are in the direction of projected areas $a_x$ and $a_y$. The drags acting on the element in $x$ and $y$ directions are $\mathbf{Q_{Dx}}$ and $\mathbf{Q_{Dy}}$ respectively.

$$\mathbf{Q_{Dx}} = C_D \cdot a_y \frac{\rho \cdot v_y^2}{2} \left[ -\frac{1}{2} \quad 0 \quad -\frac{l_e}{12} \quad 0 \quad -\frac{1}{2} \quad 0 \quad \frac{l_e}{12} \quad 0 \right]^T \tag{18}$$

$$\mathbf{Q_{Dy}} = C_D \cdot a_x \frac{\rho \cdot v_x^2}{2} \left[ 0 \quad -\frac{1}{2} \quad 0 \quad -\frac{l_e}{12} \quad 0 \quad -\frac{1}{2} \quad 0 \quad \frac{l_e}{12} \right]^T \tag{19}$$

Here, the component velocities of $v_x$ and $v_y$ and projected areas $a_x$ and $a_y$ are displayed in terms of nodal point coordinate element,

$$v_x = \frac{(\dot{e}_1 + \dot{e}_5)}{2} \tag{20}$$

$$v_y = \frac{(\dot{e}_2 + \dot{e}_6)}{2} \tag{21}$$

$$a_x = |e_1 - e_5| \cdot b \tag{22}$$

$$a_y = |e_2 - e_6| \cdot b \tag{23}$$

From above, the equation of motion of tether can be written as,

$$\mathbf{M_a\ddot{e}} = \mathbf{Q} - \mathbf{F_a} - \mathbf{F_D} + \mathbf{Q_{Dx}} + \mathbf{Q_{Dy}} \tag{24}$$

## 4. Parameter identitification technique

In the parameter identification technique, experiments are performed to identify the unknown parameters and compared to numerical analysis using Matlab/Simulink for optimum results.

### 4.1. Experimental device

With the intention of investigating the behavior of the tether in the $XY$ plane, a flat rubber is used. Additionally, the motion of rubber material which accompanies large deformation can be reproduced in a small-scale experiment. Table 1 tabulates the known parameters of the experiment. The experimental setup is illustrated in Fig. (4). The tether is included in the axis of rotation with reflector markings. The free end of the tether is located at

Table 1.

Known parameters of tether experiment

| Parameter | Symbol and unit | Value |
|---|---|---|
| Total length of tether | $l$, m | 0.6 |
| Width of tether | $b$, m | $20\times10^{-3}$ |
| Height of tether | $h$, m | $2\times10^{-3}$ |
| Cross section area | $a$, m$^2$ | $4\times10^{-5}$ |
| Second moment area | $I$, m$^4$ | $1.333\times10^{-11}$ |
| Young's modulus | $E$, N/m$^2$ | $9.4\times10^{6}$ |
| Density of tether | $\rho_t$, kg/m$^3$ | 920 |
| Density of air | $\rho$, kg/m$^3$ | 1.293 |
| Gravity acceleration | $g$, m/s$^2$ | 9.8 |

point (1,1) of the $XY$ plane and a digital video camera is used to capture its motion. Images of the markings are processed using Matlab software to investigate the behavior. So as to improve the precision of the imaging procedure, the test is performed in a dark room with infrared marking detector. The sampling time is 0.04 seconds. In this identification experiment, the catcher is fixed while the tether is in free motion from its initial raised position at angle 45°. The elastic force of the tether, drag force of air and gravity will affect the tether free fall motion.

### 4.2. Numerical analysis method

Matlab/Simulink [10] is used to analyze the motion of the tether. With the aim of assuring the reduction in computing time, the major part of the S-function program is compiled using C language. In addition, accelerator mode is set in the Simulink to provide faster calculation speed. Computing time is divided by the number of elements and changing parameters. In this case, 40 elements with a two second analysis takes about six minutes computing time. The specifications of the PC used for the calculation are, Pentium 4 with 2.80 GHz processor with 1.74 GB RAM. The numerical integration method used is Matlab Adams solver ode 113.

### 4.3. Parameter identification

The damping parameter $D$, drag coefficients $C_D$ and the number of elements $n$, are the unknown parameters that are necessary to be identified. The tether is marked with 11 equal distance points including the free end point. The evaluation function is shown as,

$$J_e = \sum_{p=1}^{f} \left[ \sum_{n=0}^{10} \left\{ \left( X_{n(p\cdot\Delta t)} - x_{n(p\cdot\Delta t)} \right)^2 + \left( Y_{n(p\cdot\Delta t)} - y_{n(p\cdot\Delta t)} \right)^2 \right\} \right] \tag{25}$$

Here, $X_{nt}Y_{nt}$ is the coordinate of each point in the tether, $x_{nt}y_{nt}$ is the coordinate of each point from numerical results, $f$ is the number of the image and $\Delta t$ is the sampling time. The time is measured for 2 seconds from the start of drop. The numerical analysis result and the experiment result are compared using this evaluation function. The parameter where the value of the evaluation function is the smallest is designated as the identification result.

In the occasion where the parameter is identified, the optimization technique is used to find local solutions. Therefore, full search is performed in order to determine the relationship between the parameter for identification

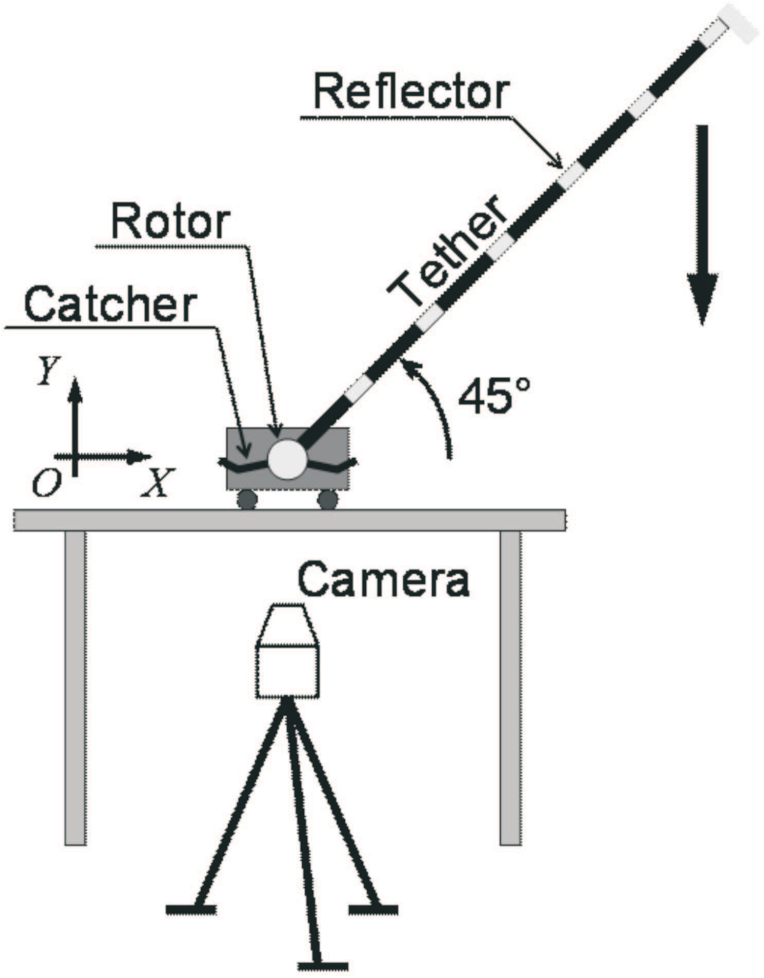


Fig. 4. Identification experiment

and evaluation function. Table 2 discloses the results of the searching. The search result in near optimal solution of 40 elements is shown in Fig. (5).

Fig. (6) reveals the minimum number of elements in each evaluation function. The value of evaluation function is small for a high number of elements. From 30 to 50 elements, the evaluation function values are about the same. Therefore, the number of elements higher than 30 is ideal for the calculation. In this case, 40 was selected for the number of elements.

Fig. (7) demonstrates the comparison of tether motion between numerical and experimental results. From free fall, the tether experienced an immediate rise at t=0.96. This almost matches with the pendulum movement repetition at a consistent pace. The motion of the flexible tether with large deformation is accurately reproduced.

Table 2.

Searching area and obtained parameters

| Symbol | Searching area | Searching step | Obtained parameters |
|---|---|---|---|
| $n$ | 10 ~ 50 | 10 | 40 |
| $D$ | 0.0 ~ 10.0×10$^3$ | 0.1×10$^3$ | 2.0×10$^3$ Ns/m$^2$ |
| $C_D$ | 0.60 ~ 0.90 | 0.05 | 0.80 |

## 5. Kinematic control

### 5.1. Swing-up control with genetic algorithm

The swing-up control inputs are generated to the target coordinate of the mass object utilizing the tether tension as well as the parameters identified earlier. The mass object attached at the free end is 21 g. In the state where tether is hung, existing gravity is acting on the tether system. The winch is moved from left to right and the tether is moved and the mass is swung up. The control rule is generated by GA.

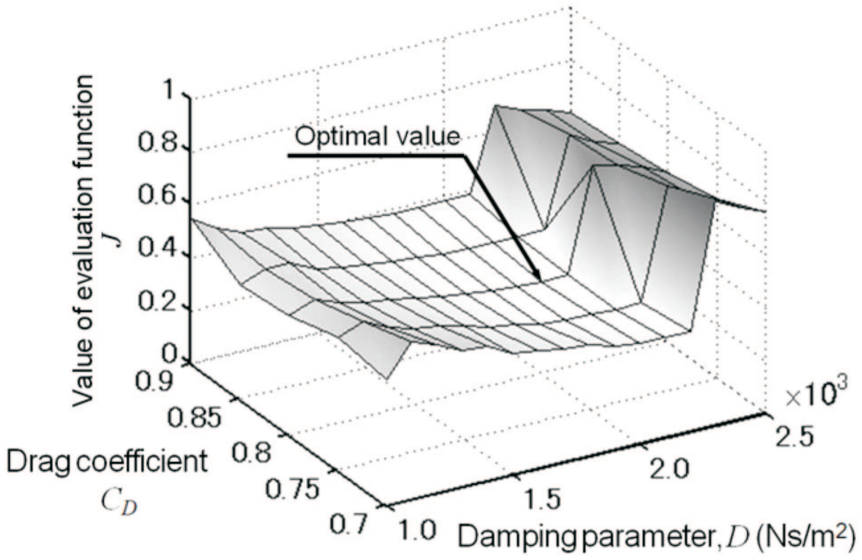


Fig. 5. Result of parameter identification (n=40)

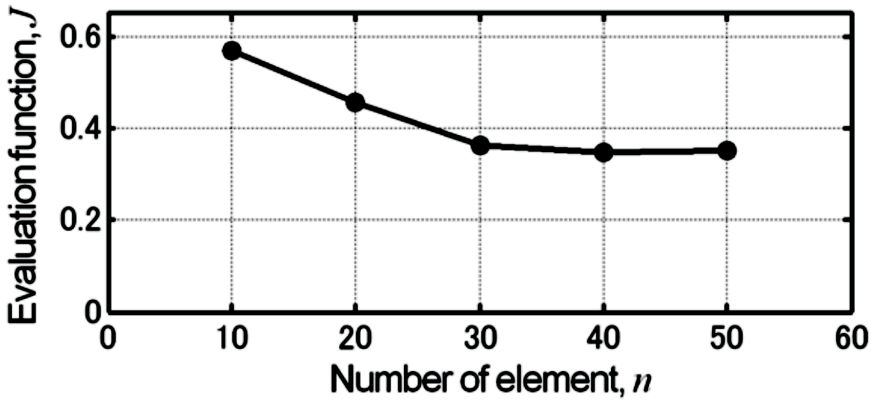


Fig. 6. Minimum value of evaluation function at each number of elements

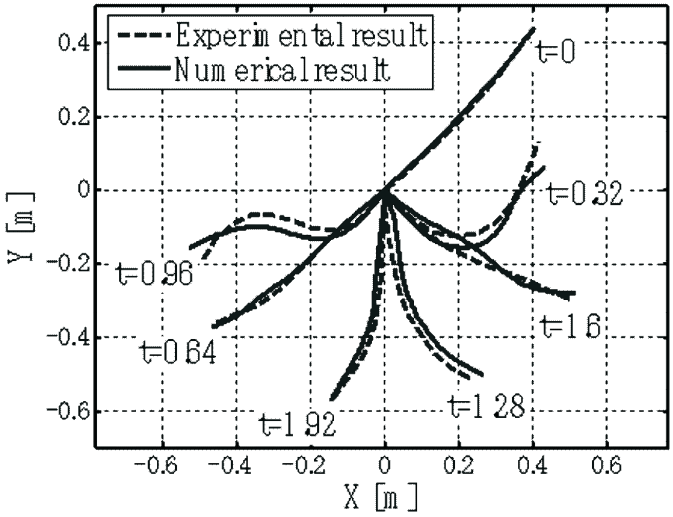


Fig. 7. Comparison between experiment and simulation of identified numerical model

In order to swing the tether up, the winch was initially moved to the left and right within the limit of 0.2 m from its initial position. The trajectory pattern captured from the experiment is represented in Fig. (8). The pattern is a combination of 3 cosine waves. The constraint of the experimental device is in an amplitude range of 0.2 m. The wave period of $T_i$ ($i$=1,2,3) and its parameter are decided by GA. $T_i$ is a 5 bit binary chromosome. One individual is a gathering of three 15 bit chromosomes. The 5 bit of binary information$XXXXX_{i(2)}$ is represented by $x_i$ and converted to a decimal number. $T_i$ is expressed as,

$$T_i = (T_{\max} - T_{\min}) \cdot \frac{x_i}{31} + T_{\min} (i = 1, 2, 3) \tag{26}$$

Here, $T_{\min} = 0.25$ s and $T_{\max} = 1.0$ s, the minimum and maximum of tracked pattern are set respectively. Within the scope of this constraint, the value is divided equally to 31 and an optimum tracked pattern of the winch is generated. The advance strategy is introduced to search the individual whose fitness is the highest with population of 10 individual per generation. The target position of the swing-up is at coordinate $(x_0, y_0)$ of the winch and tether. In order to evaluate the individual performance, the following function is used,

$$J_a(t) = \sqrt{(x_0(t) - x_n(t))^2 + (y_0(t) - y_n(t))^2} + k_1 \sqrt{\dot{x}_n^2(t) + \dot{y}_n^2(t)} + k_2 \cdot t \tag{27}$$

Here, the 1st right hand term is the distance from tether tip point $x_n y_n$ to $x_0 y_0$ and the 2nd term is the speed of the tether tip $\dot{x}_n \dot{y}_n$ and the 3rd term is the time function considered. The $k_1$ and $k_2$ are the weighting factors of 0.01 and 0.05 respectively. Using the above condition, the fitness is defined as follows,

$$J_{a\min} = \min_{t \in [\,0 \quad 3\,]} [J_a(t)] \tag{28}$$

The time needed to calculate this fitness is three second per generation which is approximately 84 minutes in real time. Fig. (9) shows the trend of fitness. Since the generation has evolved, the fitness value is decreased to constant after 17 generations. The winch track pattern obtained is displayed in Fig. (10).

### 5.2. Swing-up control with genetic algorithm

The experiment was performed to track the patterns generated by simulation and to control the position of the winch. Fig. (11) represents the absolute coordinates of the mass object of the tether tip displacement. Both numerical and experimental results agreed in regard to the mass object displacement in $x$ and $y$ directional converge in 1 s. Therefore, it is confirmed that the swing-up of the mass object at 1 s can be captured by the winch.

Fig. (12) verifies the entire motions of the tether in comparison between numerical and experimental. The shapes are well matched for all half-cosine waves. The tether underwent vibration from t=0.00 to t=0.8 due to initial

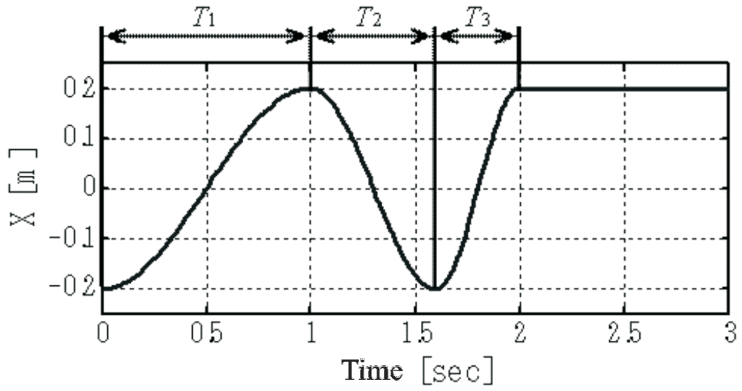


Fig. 8. Initial trajectory pattern of the winch

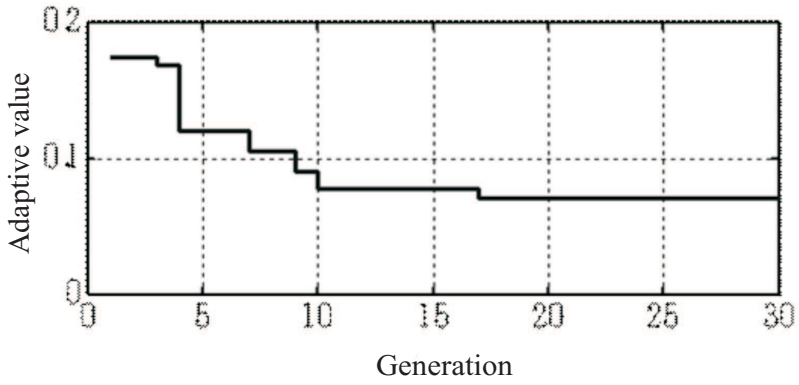


Fig. 9. Change of adaptive value of each generation

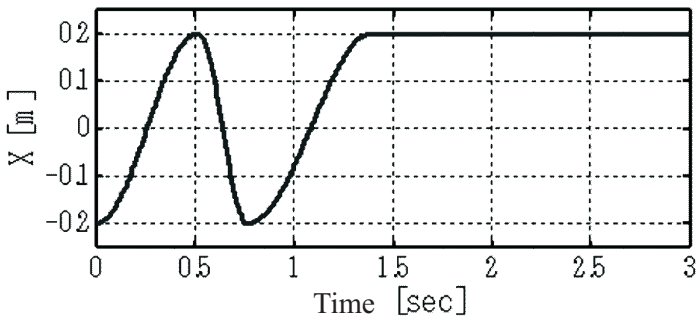


Fig. 10. Trajectory pattern of the winch obtained by GA

swing induced by the winch. The winch was moved toward the tether tip from t=0.84 onwards. At t=1.00, the capture is confirmed as the mass object landed on the catcher.

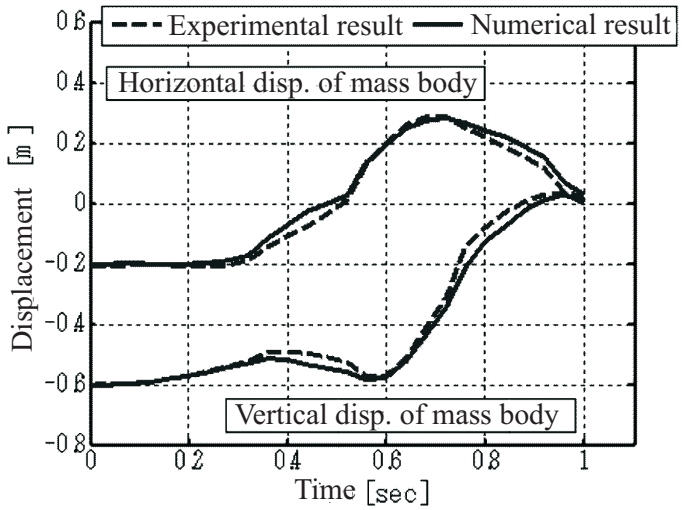


Fig. 11. Time response of mass body displacement

## 6. Conclusion

In this report, the formulation and identification technique in consideration of the damping force with ANC method for tether motion accompanying large deformation is proposed. The kinematics control experiment of tether system is performed with control rule construction utilizing the precise multibody dynamics model. The damping force and drag force acting on the tether are formulated based on ANC method. The numerical simulation model of the tether system has been validated by the experiment to identify quantitatively of the damping parameter, drag force coefficient and number of element partitions. The genetic algorithm control rule approach is used to demonstrate the swing up control and the capture of the mass object of the tether system. The swing-up control experiment's actual capture of the mass object verified the control rule generated by numerical analysis. The practicality and availability of the tether model using flexible body dynamics and kinematics control of the tether system using genetic algorithm were established successfully.

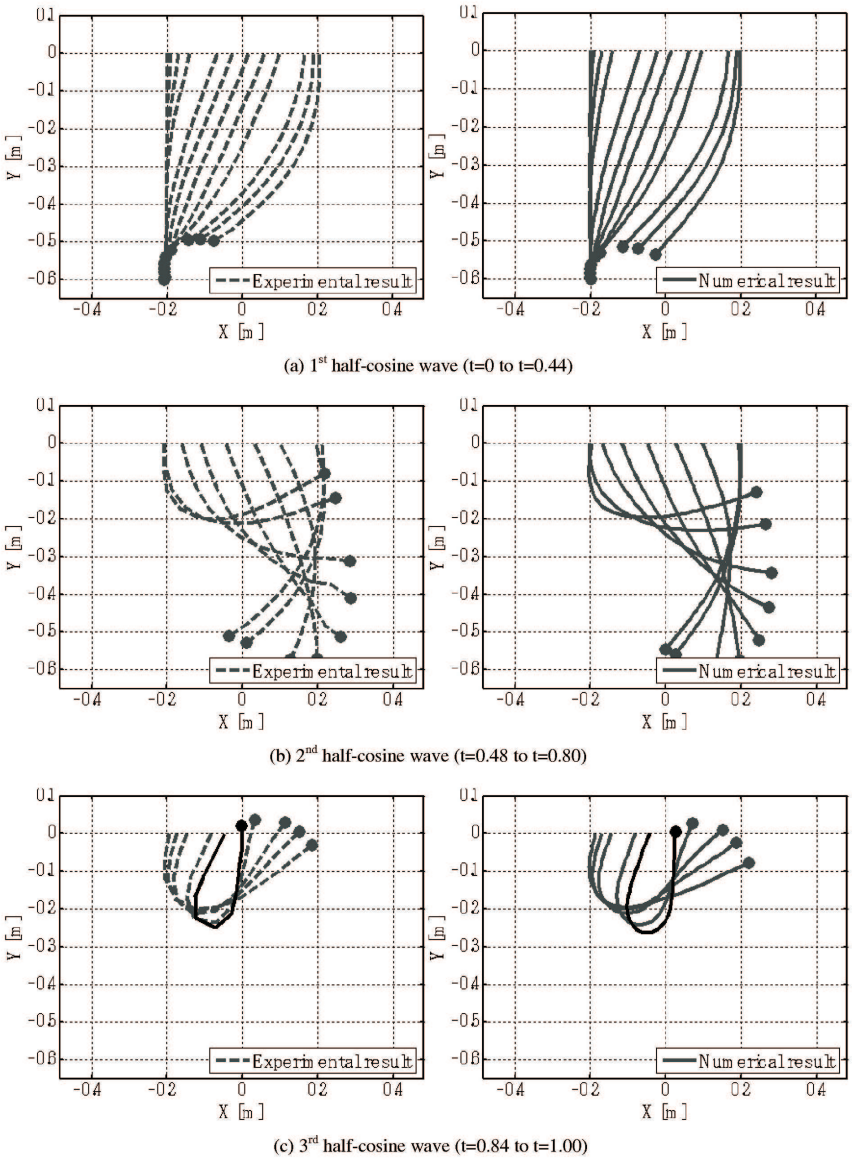


(a) 1st half-cosine wave (t=0 to t=0.44)

(b) 2nd half-cosine wave (t=0.48 to t=0.80)

(c) 3rd half-cosine wave (t=0.84 to t=1.00)

Fig. 12. Experimental result and numerical result of swing-up control

The author (Mohd Azman Abdullah) would like to acknowledge financial support from the Ministry of Higher Education of Malaysia and Universiti Teknikal Malaysia Melaka under the SLAI financial scheme.

Manuscript received by Editorial Board, December 10, 2009;
final version, February 05, 2010.

REFERENCES

[1] Nohmi N., Yoshida S.: Experimental analysis for attitude control of a tethered space robot under microgravity. Space Technology, **24**, 119-128, 2004.
[2] Nohmi M., Nenchev N. D., Uchiyama M.: Motion control of a tethered space robot during casting. Transactions of the Japan Society of Mechanical Engineers, Series C, **66**, 2255-2261, 2000.
[3] Takehara S., Terumichi Y., Nohmi M., Sogabe K.: Numerical and experimental approaches on the motion of a tethered system. Journal of System Design and Dynamics, **2**, 1106-1117, 2008.
[4] Shabana A. A., Hussien A. H., Escalona L. J.: Application of the absolute nodal coordinate formulation to large rotation and large deformation problems. Journal of Mechanical Design, **120**, 188-195, 1998.
[5] Shabana A. A.: Dynamic of multibody system 3rd edition. Cambridge University Press, New York, 2005.
[6] Takahashi Y., Shimizu N., Suzuki K.: Study on the damping matrix of the beam element formulated by absolute nodal coordinate approach. Transactions of the Japan Society of Mechanical Engineers, Series C, **69**, 2225-2232, 2003.
[7] Takahashi Y., Shimizu N.: Study on the elastic force for the deformed beam by means of the absolute nodal coordinate multibody dynamics formulation (Derivation of the elastic force using finite displacement and infinitesimal strain). Transactions of the Japan Society of Mechanical Engineers, Series C, **67**, 626-632, 2001.
[8] Takehara S., Terumichi Y., Nohmi M., Sogabe K.: Motion of a system consisting of a string and rigid bodies as its end, Transactions of the Japan Society of Mechanical En-gineers, Series C, **69**, 349-355, 2003.
[9] Sivanandam S. N., Deepa S. N.: Introduction to genetic algorithms. Springer, Berlin, 2007.
[10] Beucher O., Weeks M.: Introduction to matlab & simulink: a project approach. Infinity Science Press, New Delhi, 2008.

**Sterowanie wychyleniem masywnego ciała na elastycznej uwięzi**

Streszczenie

Systemy z uwięzią znajdują zastosowanie m.in. w technice satelitarnej, gdzie statek-matka i osprzęt satelitarny są złączone liną. By szczegółowo opisać ruch tego rodzaju układów, można modelować uwięź jako ciało elastyczne i stosować w obliczeniach metodę układów wieloczłonowych. W analizie i modelowaniu ciała podatnego – uwięzi, należy brać pod uwagę znaczne odkształcenia i przemieszczenia. By opisać dynamikę ciała podatnego można wykorzystać metodę układów wieloczłonowych, stosując sformułowanie w bezwzględnych współrzędnych węzłowych (Absolute Nodal Coordinate Formulation) i wprowadzając siły tłumienia. Celem weryfikacji metody modelowania, w przedstawionym studium proponuje się eksperymentalne podejście do identyfikacji parametrów. Przykładowe sterowanie wychyleniem, w którym wykorzystano genetyczny algorytm sterowania, zostało wykonane na drodze symulacji i eksperymentalnie. Zgodność modelu z rzeczywistością i użyteczność sterowania ruchem na podstawie analizy dynamiki układu wieloczłonowego zostały pokazane poprzez porównanie symulacji numerycznej i danych eksperymentalnych.